Environ. Sci. Technol. **1999**, *33,* 1825−1831

A Predictive Model for Adsorptive Gas Partitioning of SOCs on Fine Atmospheric Inorganic Dust Particles

MYOSEON JANG AND
RICHARD M. KAMENS*

Department of Environmental Sciences and Engineering, CB 7400, Rosenau Hall, The University of North Carolina at Chapel Hill, Chapel Hill, North Carolina 27599-7400

The adsorptive gas/particle (G/P) partitioning of semivolatile organic compounds (SOCs) on inorganic Arizona road dust was studied using outdoor Teflon film chambers. Physicochemical parameters from SOC molecular structural information were implemented to describe nonspecific and specific interactions relating to G/P adsorption. Experimental partitioning data were successfully interpreted using physicochemical parameters such as vapor pressure, molecular polarizability, and solute solvation. To evaluate the effect of surface functional groups on the adsorptive G/P partitioning of SOCs, untreated and baked Arizona road dust particles were used. The partitioning coefficients, K_p, for a range of different SOCs on baked dust particles and on untreated dust particles were measured from simultaneous experiments in two outdoor Teflon film chambers that were operated at the same temperature and humidity conditions. K_p values for the two different surface properties of untreated and baked particles were better predicted by including solute solvation parameters than just by vapor pressure alone.

Introduction

Recently, absorptive gas/particle (G/P) partitioning of semivolatile organic compounds (SOCs) has received much attention. However, our understanding of the fundamental theory associated with the adsorptive partitioning of SOCs is limited, even though dry deposition onto adsorptive particle surfaces is an important environmental removal pathway for SOCs. The chemical structures of most environmental adsorbents include a large number of different molecular functionalities or configurations, and their surfaces are heterogeneous (*1*). Unlike volatile organic compounds (VOCs), which have often been manipulated by gas chromatography (*2*, *3*), adsorptive partitioning studies of SOCs on gas chromatographic substances at ambient temperatures are scarce due to their low volatility.

For more than a decade, adsorptive SOC equilibrium between a gas phase and a particle surface has been expressed as a function of vapor pressure. Pankow and co-workers (*4*−*10*) were able to relate an atmospheric adsorptive G/P partitioning coefficient, K_p, to SOC vapor pressures, energies of sorption, particle surface area, and the number of surface sorption sites. For any given compound at a given temperature, K_p is described by

$$\log K_p = \log\frac{F}{A \times \mathrm{TSP}} = \log (N_s A_{tsp} T/16) + (Q_l - Q_v)/(2.303RT) - \log p_L^\circ \quad (1)$$

where F is the SOC particle-phase concentration (in ng/m^3), A is the gas-phase concentration (in ng/m^3), TSP is the concentration of total suspended particulate matter in the atmosphere (in μg/m^3), A_{tsp} (cm^2/μg) is the specific surface area of the particulate matter, N_s (mol/cm^2) is the surface concentration of sorption sites, Q_l (J/mol) is the enthalpy of desorption for an SOC from the surface, Q_v (J/mol) is the enthalpy for vaporization of an SOC from the subcooled liquid, R is the gas constant (8.314 J mol^{-1} K^{-1}), T (K) is the temperature, and p_L° (Torr) is the vapor pressure of a subcooled liquid.

In gas−solid interface interactions, Q_l reflects the strength of attraction between an SOC and active sites on a surface and is closely related to the mean residence time for adsorption or a K_p value (*11*). At a given temperature, the $(Q_l - Q_v)/(2.303RT)$ term in eq 1 expresses the net interaction between desorption and condensation for a pure compound and varies with either the chemical nature of surfaces or chemical functional groups of SOCs. From the above discussion, a further understanding of either Q_l or $(Q_l - Q_v)$ using physicochemical parameters (based on the thermodynamic properties of SOCs) may permit one to interpret the properties of the adsorptive partitioning coefficient of SOCs on solid particulate matter.

Goss (*12*−*17*) has developed a predictive model for adsorption of different organic compounds on different surfaces, based on the excess free energy of adsorption, which consists of two different interactions: van der Waals interactions and Lewis acid−base interactions. In this model (*12*−*17*), the adsorption of volatile organic compounds was carried out using a chromatographic method, and adsorptive coefficients for either different compounds or surfaces have been successfully interpreted using physicochemical parameters related to these two basic interaction energies (*16*, *17*).

The quantitative physicochemical scales most frequently used to describe the nature of a medium have been developed for gas chromatographic systems to describe the behavior of a solute between the gas and condensed phases. The physicochemical parameters that are obtained from molecular properties can also be used to explain experimental G/P partitioning coefficients observed in outdoor smog chambers.

Polarity scales from a linear solvation energy relationship (LSER) were developed by Kamlet and Taft using the empirical solvatochromic processes of nonassociated liquids (*18*−*27*) and have been extended to other types of solute systems by Abraham and co-workers (*3*, *28*−*32*). This permits the prediction of a set of retention data for a given chromatographic system, retention volumes (log V_G) for different solvents on a given condensed phase, and gas−liquid chromatographic (GLC) partitioning coefficients (log L). The partitioning coefficients are the ratio of a solute concentration in solution to a solute concentration in the gas phase (*28*).

Since partitioning to a chromatographic column is similar to atmospheric G/P partitioning, it is expected that the polarity scales developed by Abraham can also be applied to the atmospheric G/P partitioning coefficient, K_p, with the following form:

$$\log K_p = c_1 + r_1R_2 + s_1\pi_2^H + a_1\alpha_2^H + b_1\beta_2^H + l_1 \log L^{16} \quad (2)$$

* Corresponding author e-mail: kamens@unc.edu; telephone: (919)966-5452.

10.1021/es9805167 CCC: $18.00
Published on Web 04/21/1999

TABLE 1. Conditions for Outdoor Smog Chamber Experiments Using Fine Arizona Road Dust

date	particle sources	chamber[a]	temp (K)	RH[b] (%)	TSP (μg/m^3)
Oct 26, 1996	untreated particles	190 m^3	289−287	99	700−270
Dec 11, 1997	untreated particles	25 m^3 (E)	285−280	76−94	5070−2460
Dec 11, 1997	baked particles	25 m^3 (W)	285−280	76−94	3190−1810

[a] W and E denote the west and east chamber. [b] RH is relative humidity.

The descriptors in eq 2 are as follows: R_2, the solute excess molar refraction; π_2^H, the solute dipolarity/polarizability; α_2^H, the solute Lewis acidity; β_2^H, the solute Lewis basicity; and log L^{16}, the gas−liquid partitioning coefficient of a solute in hexadecane (*28*−*32*). R_2, π_2^H, and L^{16} are used for estimating solute scales for either non-hydrogen bonding or nonaromatic solvents. The R_2 parameter is an explanatory variable that refers to a specific type of solute−solvent phase interaction via π or n-electron pairs, and L^{16} is used to account for general dispersional interactions between a solute and a medium. The solvatochromic π_2^H polarity scale is an index of liquid dipolarity and polarizability, which measures the ability of a liquid to stabilize a charge or dipole according to its dielectric effect. α_2^H and β_2^H are employed to modify specific interactions such as a hydrogen bonding interactions. The effectiveness of α_2^H and β_2^H for a given solute is determined by the properties of active sites on the surface of condensed matter. c_1 is a constant, and r_1, s_1, a_1, b_1, and l_1 are regression coefficients.

In this study, the adsorptive model advanced by Goss was applied to the atmospheric adsorptive G/P partitioning of different polarity SOCs on ambient inorganic particulate matter. Outdoor chamber experiments were conducted to demonstrate the applicability of a semiempirical predictive model using this LSER method. Two different types of realistic particle systems, untreated Arizona road dust particles and baked (referred to here as modified) Arizona road dust particles, were used to evaluate the influence of surface properties on G/P adsorption of SOCs. Partitioning coefficients, previously treated with a simple log K_p vs log p_L° relationship were successfully modified with the use of other physicochemical parameters.

Experimental Section

The adsorption of SOCs on fine inorganic Arizona road dust (supplied by the former AC Spark Plug Division of the General Motors (GM) Corporation, Flint, MI) was investigated in a 190 m^3 and two 25 m^3 outdoor Teflon film chambers (*33, 34*). All experiments were carried out in the dark to exclude photochemical reactions. Arizona road dust was injected into the outdoor smog chambers via a high-pressure venturi aerosol generator. The particle concentrations, temperature, and humidity for the three outdoor chamber experiments used in this study are shown in Table 1. Dust injection was followed by the simultaneous addition of a mixture of 18 SOCs to the gas-phase atmosphere of the chamber (*33, 34*). SOCs included alkanes, alkanoic acids, polynuclear aromatic hydrocarbons (PAHs), oxygenated PAHs, and nitro PAHs. The two 25 m^3 chambers, designated as east and west chambers, were used simultaneously for untreated and modified dust experiments on December 11, 1997, to address different surface effects on G/P partitioning of SOCs. In these experiments, modified dust particles that were previously baked at 700 °C for 4 h were used in one chamber, while untreated dust particles were directly injected into the other chamber. Particle sizes were monitored with a laser optical aerosol instrument (0.3−20 μm, LAS-X, Particle Measuring System Inc., Boulder, CO). After injection of particles into each chamber, a period of 3−5 h was required to permit settling of large dust particles. At this point, about 93% of the surface area, as calculated from the experimentally measured particle distribution, was associated with particles less than 2.5 μm in diameter. The chamber particle distribution of Arizona road dust was not changed by the baking process.

The G/P phase sampling train consisted of an upstream 40-cm 5-channel annular denuder to collect gas-phase SOCs. This was followed by a 47-mm Teflon glass fiber filter (type T60A20, Pallflex Products Corp., Putnam, CT) to collect particles and their sorbed SOCs and by another 5-channel denuder to collect particle-phase SOCs released from the particles during sampling. The concentrations of SOCs in gas-particle phases were analyzed by gas chromatography−mass spectrometry (GC−MS) using a Hewlett-Packard 5890 gas chromatograph interfaced with a Hewlett-Packard 5971A mass selective detector. Details of the sampling and workup procedures and analytical precision have been reported in other manuscripts (*33, 34*). The modification of functional groups on the surface of the dust particles due to baking at 700 °C and the loss of particle-bound water was characterized by FT-IR. Infrared spectra of dust particles were obtained with a Mattson Polaris TM infrared spectrometer in the absorbance mode, and samples were prepared in KBr pellets.

Results and Discussion

Arizona Inorganic Road Dust Particles. Arizona road dust was used by the automobile industry to challenge carburetor air filters. Since Arizona road dust was well characterized according to its particle size and elemental composition, a number of aerosol investigators have used it as a standard material for inorganic aerosol studies. Its density is 2.4 g/cm^3, and the listed elemental analysis for Arizona road dust particles by GM was Si (45.9%), Ca (17.3%), Mg (14.6%), Al (12.4%), Fe (5.9%), and K (3.78%). This analysis suggests that the main components of Arizona road dust are silica and silicates, followed by smaller fractions of aluminum and magnesium oxide. Inorganic dust such as soil debris contains very low extractable organics when extracted with organic solvents. This implies that partitioning of SOCs onto these surfaces occurs predominantly by gas−surface adsorptive processes.

Arizona road dust particles were modified by baking at 700 °C to evaluate the adsorptive partitioning of SOCs on different kinds of surfaces. The alteration of functional groups was characterized by FT-IR. Figure 1 shows FT-IR spectra for untreated and baked dust. Spectra of either untreated or baked Arizona road dust exhibit a strong Si−O silica stretching in 1300−1000 cm^{-1} (*35*). The broad adsorption band between 3700 and 3100 cm^{-1} is associated with O−H stretching from surface-bound water molecules and hydroxyl groups (*35*). After baking the dust particles for 4 h at 700 °C, the O−H stretching bands disappeared (Figure 1), indicating that hydroxyl groups and bounded water molecules were driven from the dust particles during the baking process of inorganic dust particles. FT-IR spectroscopy, however, has limitations for the surface characterization with respect to the surface water uptake at ambient humidities, because it only provides functional group information for the averaged bulk composition of the dust particles. It is reasonable to assume,

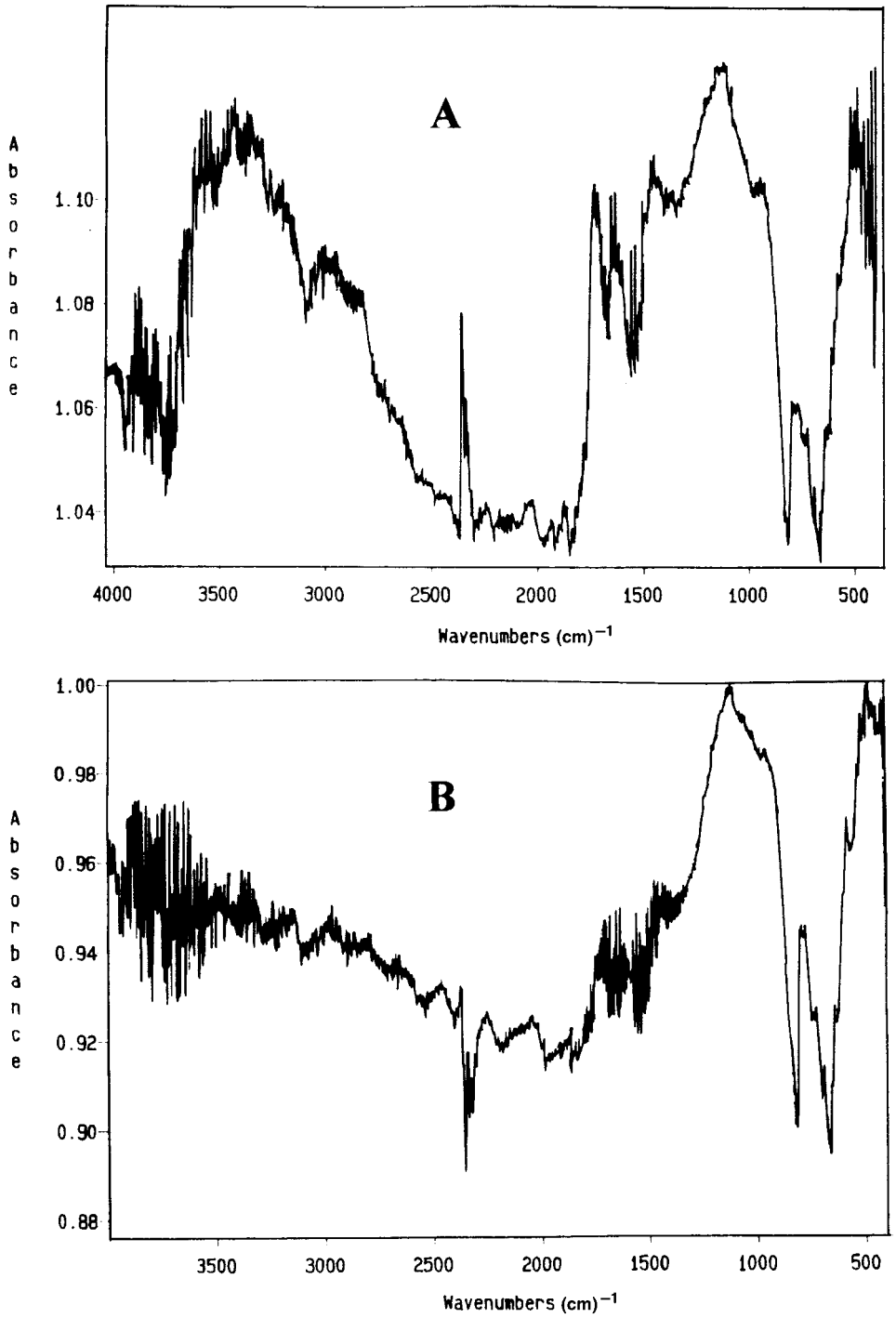

FIGURE 1. FT-IR spectra for fine Arizona road dust particles in KBr pellet: untreated dust particles (A) and baked dust particles for 4 h at 700 °C (B).

however, that baking will drive water from the surface of particles before it is lost from the particle interior. Oxides or hydroxyl groups on inorganic particle surfaces are the active sites for the adsorption of SOCs and water molecules, and their distribution is geometrically heterogeneous (*36*). Water adsorption may occur differently for untreated and baked dust particles, and sorbed water has highly mixed monolayer/multilayer properties on active sites beyond a certain partial pressure of water.

Properties of the Interaction Energy in Adsorptive G/P Partitioning. The fundamental description for non-self-associated adsorption of organic compounds originates from nonspecific interactions. These interactions are characterized by dispersional and dipole interactions between an adsorbent surface and an organic molecule. Molecular induction polarizability (α) is the common parameter used to represent the dispersional force of nonspecific interactions. Table 2 lists the SOCs used in this study along with their molecular polarizabilities. When literature values were unavailable, α values were calculated by the additive technique developed by Miller and Savchik (*37*, *38*). The most successful empirical approaches estimate an average molecular polarizability based on the environment through which atomic hybridization occurs around a central atom defining a bond or functional group. Miller and Savchik tabulated the atomic hybrid component for each atom A, τ_A(ahc), using an empirical additive method (*37*, *38*). In Figure 2, molecular polarizabilities (α values) of SOCs are plotted vs experimental

TABLE 2. Physicochemical Parameters of SOCs

no.	SOCs	log p_L° 288 K[a]	log(10³ K_p)[m] 288 K ($m^3/\mu g$)	log p_L° 282 K[a]	log(10³ K_p)[n] 282 K ($m^3/\mu g$)		α ($Å^3$)	R_2	π_2^H	α_2^H	β_2^H	log L^{16} 298 K	$^i\gamma^\infty{}_{16}$[e]	ref
P1	fluorene	ni[o]		−3.21	−2.52	−2.44	21.7[b]	1.59	1.03	0	0.2	6.92	0.43	31, 32
P2	phenanthrene-d_{10}	−3.72	−2.69	−4.00	−1.60	−1.67	24.7[b]	2.1	1.29	0	0.26	7.63	0.54	31, 32
P3	anthracene	−3.78	−2.46	ni	ni	ni	25.4[b]	2.29	1.34	0	0.26	7.57	0.54	31, 32
P4	anthracene-d_{10}	−3.75	−2.47	ni	ni	ni	25.4[b]	2.29	1.34	0	0.26	7.57	0.54	31, 32
P5	fluoranthene	−4.81	−1.07	−5.13	−0.35	−0.49	28.3[b]	2.38	1.71	0	0.29	8.63	0.74	31, 32
P6	pyrene	−5.01	−1.17	−5.33	0.05	−0.28	29.3[b]	2.81	1.71	0	0.29	8.83	0.74	31, 32
P7	pyrene-d_{10}	−4.99	−0.98	−5.32	0.05	−0.36	29.3[b]	2.81	1.71	0	0.29	8.83	0.74	31, 32
P8	benz[*a*]anthracene	−6.34	0.19	−6.71	1.00	0.88	32.9[b]	2.99	1.7	0	0.32	9.98	0.8	31, 32
P9	9-methylanthracene	−3.93	−1.69	ni	ni	ni	26.9[c]	2.29	1.34[j]	0	0.26	7.71	0.54	31, 32
AL1	heptadecane-d_{36}	−3.57	−2.51	ni	ni	ni	33.9[c]	0	0.05	0	0	8.22	0	31, 32
AL2	nonadecane-d_{40}	−4.59	−1.21	−4.79	−0.26	−0.76	37.6[c]	0	0.05	0	0	9.23	−0.01	31, 32
AL3	eicosane-d_{42}	−5.27	−0.61	−5.62	0.37	0.14	39.4[c]	0	0.05	0	0	9.73	−0.01	31, 32
AL4	tricosane-d_{48}	ni	ni	−6.83	1.17	0.87	43.1[c]	0	0.05	0	0	11.25	−0.03	31, 32
AD1	dodecanoic acid	−5.48	1.01	−6.06	1.98	1.43	23.5[c]	0.083	0.45	0.6	0.45	7.19	0.52	31
O1	4-biphenylcarbaldehyde	−3.67	−1.15	−3.96	−1.34	−1.43	24.6[b]	un[p]	1.48[f]	0[g]	0.39[g]	7.02[d]	0.98	32
O2	9-phenanthrenecarbaldehyde	−5.21	0.27	−5.54	0.59	0.45	26.9[c]	un	1.78[f]	0[g]	0.39[g]	8.49[d]	0.98	32
O3	9,10-anthraquinone	−5.19	−0.89	−5.52	1.08	0.92	24.5[b]	1.405	1.5[h]	0[h]	0.5[h]	8.44[d]	1.01	31
O4	3,5-dimethylphenol	ni	ni	−1.93	−3.08	−2.95	14.7[c]	0.82	0.84	0.57	0.36	4.86	1.01	32
O5	2-isopropyl phenol	ni	ni	−1.67	−2.98	−3.04	15.6[c]	0.793[i]	0.88[i]	0.52	0.37[i]	5.19	0.9	30, 32
O6	BHT	−2.79	−1.63	−3.80	−2.52	−1.68	27.6[c]	0.86	0.79[i]	0.37	0.2[i]	6.35[d]	0.79	30, 32
O7	nonylphenol	ni	ni	−2.58	−2.17	−2.04	27.6[c]	un	0.88[i]	0.55[i]	0.37[i]	5.85[d]	0.79	32
N1	9-nitroanthracene	ni	ni	−6.44	0.98	1.00	26.1[c]	un	1.94[k]	0[l]	0.28[l]	9.51[d]	0.81	32

[a] Refs *4−10, 33,* and *40−44.* [b] Experimental data from literature (*37, 38*). [c] By calculation (*37, 38*). [d] Log $L^{16} = -\log p_L^\circ - \log {}^i\gamma^\infty{}_{16} + \log (7.501RT/MW_{16})$ (*33*). [e] UNIFAC calculation (*33*). [f] π_2^H(unsubstituted) + [π_2^H(benzaldehyde) − π_2^H(benzene)]. [g] From bezaldehyde. [h] From benzophenone. [i] From 4-*n*-propylphenol. [j] From 2,6-dimethylphenol. [k] π_2^H(anthracene) + [π_2^H(nitrobezene) − π_2^H(benzene)]. [l] From nitrobenzene. [m] Experiments on October 27, 1996, at 99% RH. [n] Experiments on December 11, 1997 at 77% RH. [o] ni, not injected into the chamber. [p] un, unknown.

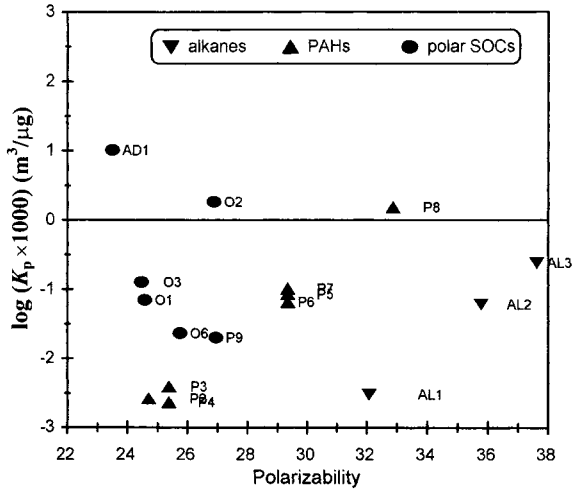

FIGURE 2. Correlation of experimental log K_p values vs molecular polarizability (α) for various semivolatile organic compounds (SOCs) on fine Arizona road dust particles (October 27, 1996). The experimental temperature was 288 K, and the relative humidity was 99%. See Table 2 for compound identities.

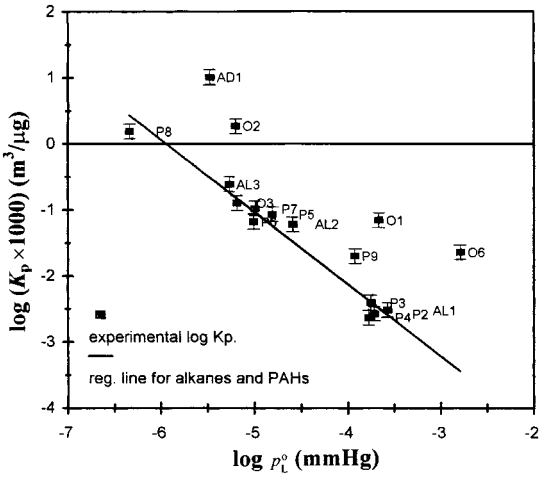

FIGURE 3. Log K_p values vs log p_L° correlation for various semivolatile organic compounds (SOCs) on fine Arizona road dust particles (October 27, 1996). The experimental temperature was 288 K, and the relative humidity was 99%. The solid line is an idealized plot for log K_p values vs log of nonpolar SOCs, alkanes, and PAHs (slope = −1.09 and r^2 = 0.97). Compound identities are given in Table 2.

log K_p values for SOCs in the presence of inorganic Arizona dust particles (October 27, 1996). For a homologous series of alkanes and PAHs, experimental log K_p values are linearly correlated with α values. The parallel gap between PAHs and alkane homologous series results from differences that are not characterized completely by the dispersional interactions. Adsorption of alkanes on dust particles is mostly maintained by dispersional interactions, while PAHs have some additional sorption interactions resulting from the interaction of aromatic π electrons with the active sites on dust surfaces (*39*). Other SOCs, which contain strong hydrogen-bonding interactions with surface-active sites, are additionally displaced from the linear correlation lines for both alkanes and PAHs (Figure 2).

In the past, nonspecific adsorptive G/P partitioning has been described as a direct function of log p_L° (*4−8*). Linearity between log K_p and log p_L° has been observed for a homologous series of alkanes, chlorinated organics, and PAHs in ambient air and chamber studies (*4−8*). This approach is most successful in describing the partitioning of nonpolar compounds. However, if one considers compounds with different polarities and functional groups, a direct relationship between log K_p and log p_L° is not sufficient to describe considerable contributions from other interactions such as hydrogen bonding of SOCs to an adsorbent.

Figure 3 shows the correlation of log K_p vs log p_L° for partitioning of SOCs on inorganic Arizona dust particles (October 27, 1996). Vapor pressures of SOCs (*4−10, 40−44*) used in outdoor smog chamber experiments are listed in Table 2. When the correlation of log K_p vs log p_L° was applied to the alkane and PAH homologous series, a reasonable linear

relationship was observed with a slope of −1.09 and an r^2 of 0.97 (Figure 3). Polar SOCs with hydroxyl, carboxylic acid, and carbonyl functionalities however deviated considerably from the correlation line of log K_p vs log p_L° for nonpolar SOCs. When all polar and nonpolar SOCs are included in the log K_p vs log p_L° relationship, the r^2 dropped to 0.63 and the slope decreased to −0.91. This suggests, as expected, that the adsorption energy of polar SOCs on this mineral adsorbent may differ greatly from the condensation energy (Q_v) of a pure SOC on itself. This results from the strong interaction of polar SOCs with surface-active sites.

Application of a Solute Scale for Hydrogen Bonding in Adsorptive Partitioning. The same physicochemical parameters employed to scale the adsorption of a solute on chromatographic column substrates (*3*) are also applicable to semiempirical predictive models for the atmospheric adsorption of SOCs on ambient inorganic particulate matter. In addition to nonspecific interactions, the LSER approach (eq 2 above) contains descriptors for specific interactions such as acid−base interactions. Including these parameters can provide improved predictability for the adsorptive gas partitioning on particulate matter.

Because R_2 values of some SOCs are not available in the literature, the molecular polarizability (α) of SOCs, which can be estimated easily by additivity (*37, 38*), was substituted for R_2 in eq 2. Thus

$$\log K_p = c_2 + r_2\alpha + s_2\pi_2^H + a_2\alpha_2^H + b_2\beta_2^H + l_2 \log L^{16} \quad (3)$$

where again c_2 is a constant and r_2, a_2, s_2, b_2, and l_2 are regression coefficients. The log L^{16} term, which accounts for the dispersional interaction of a solute−column system, can be expressed as $-\log p_L^\circ - \log {}^i\gamma^\infty_{16} + \log (7.501RT/MW_{16})$, where ${}^i\gamma^\infty_{16}$ is the activity coefficient of an SOC (i) in hexadecane at infinite dilution and MW_{16} is the molecular weight of hexadecane (*33*). Over a range of ambient temperatures, the log $(7.501RT/MW_{16})$ term can be regarded as a constant. Thus, including the log p_L° term, eq 3 gives

$$\log K_p = c_3 + r_3\alpha + s_3\pi_2^H + a_3\alpha_2^H + b_3\beta_2^H + v_3 \log p_L^\circ + g_3 \log {}^i\gamma^\infty_{16} \quad (4)$$

The log ${}^i\gamma^\infty_{16}$ values of solutes are calculated by a group contribution method (*33*) and are listed in Table 2 along with other physicochemical parameters. The ${}^i\gamma^\infty_{16}$ value represents the nonideality of an SOC in hexadecane, which is a typical nonpolar medium characterized primarily by dispersional interactions. The log ${}^i\gamma^\infty_{16}$ term conceptually characterizes other interactions that exceed typical dispersional interactions and is strongly associated with the solute scales, R_2, π_2^H, α_2^H, and β_2^H. Inclusion of the log ${}^i\gamma^\infty_{16}$ term into these parameters transforms eq 4 to

$$\log K_p = c_4 + r_4\alpha + s_4\pi_2^H + a_4\alpha_2^H + b_4\beta_2^H + v_4 \log p_L^\circ \quad (5)$$

Here, excess energies of adsorption are explained with the terms α, π_2^H, α_2^H, and β_2^H.

When the $(Q_l - Q_v)$ term in eq 1 behaves as a constant, the effect of temperature on K_p for atmospheric adsorptive partitioning can be essentially illustrated by the log K_p vs log p_L° relationship because log p_L° varies as $1/T$. However, $(Q_l - Q_v)$ varies from compound class to class. The interaction energy between a molecule and a surface of a solid particle is regarded as the sum of molecular interactions with all the molecules on a solid surface (*45*). Even when the geometry changes, the basic interaction energies are additive. The $Q_l - Q_v$ term in eq 1, the energy difference between condensation of a pure SOC and the adsorption of an SOC on surfaces, may be viewed as corresponding to the solute scales in eqs 2−5. Given that the α, π_2^H, α_2^H, and β_2^H terms now specifically represent the $Q_l - Q_v$ term in eq 1, the constant c_4 in eq 5 should contain a contribution of A_{tsp} (cm²/μg), the specific surface area of the particulate matter.

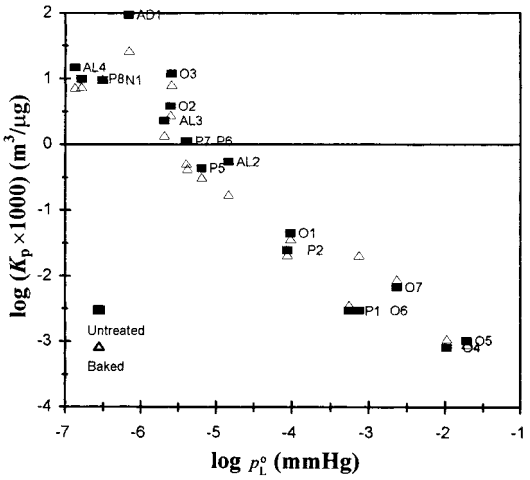

FIGURE 4. Experimental log K_p values vs log p_L° correlation for various semivolatile organic compounds (SOCs) on two different kinds of fine Arizona road dust particles (December 11, 1997): untreated and baked. The temperature was 282 K, and the relative humidity was 77%. Identification numbers correspond to SOCs listed in Table 2.

Wet vs. Dry Chamber Experiments. Experimentally determined log K_p values from a dual outdoor 25 m^3 chamber experiment with untreated and baked dust particles (December 11, 1997) are plotted vs their calculated log p_L° values in Figure 4. Table 3 summarizes the correlation coefficients for eqs 3 and 5. Experimental log K_p values for 18 SOCs are empirically fitted with physicochemical parameters (Table 2) for the untreated and modified fine inorganic Arizona dust particles.

Equations 3 and 5 can also be simplified using just the statistically significant terms that contribute to the regression analysis. A statistical package (SAS, version 6.12) was employed for these stepwise forward regressions. It was initiated with either log p_L° or log L^{16} because these are most highly correlated with log K_p values. The partial F statistics associated with each remaining variable based on regression equations containing that variable and variables selected in a pre-stepwise regression were calculated and tested (at level $\alpha = 0.05$). Table 3 gives the correlation coefficients for the simplified equations, which consist of the statistically significant terms. In Table 3, these simpler equations are called eqs 5-1, 5-2, 5-3, etc. and contain the following terms: log p_L°, π_2^H, α_2^H, and β_2^H for eq 5-1; log L^{16}, α_2^H, and β_2^H for eq 3-2; log p_L°, α_2^H, and β_2^H for eq 5-2; log L^{16}, π_2^H, and β_2^H for eq 3-3; log p_L°, π_2^H, and β_2^H for eq 5-3. The π_2^H, α_2^H, and β_2^H parameters were potentially susceptible to hydrogen bonding at surface-active sites, while the dispersional parameter (the polarizability term in eqs 3 and 5) was neither affected by the active sites of the dust surfaces nor was it statistically significant. To predict partitioning coefficients of SOCs, π_2^H, α_2^H, and β_2^H parameters along with either log L^{16} or log p_L° were statistically important and gave reasonable predictions for realistic inorganic dust surfaces. α_2^H and β_2^H parameters are needed because the hydrogen-bonding interactions of self-associated SOCs would be underestimated on dust surfaces by just using either log L^{16} or log p_L°. A plot of experimental log K_p values vs predicted log K_p values using eq 5 is illustrated in Figure 5. An almost identical plot is obtained using eq 5-3 in Table 3, which just uses the three terms log p_L°, π_2^H, and β_2^H for 18 data points. Although more data points are desirable to strengthen the statistical power of the regression analysis

TABLE 3. Correlation Coefficients for Experimental Log K_p Values of SOCs on Fine Arizona Road Dust Particles (December 11, 1997) Using Regression eqs 3 and 5

particles	eq	no. of terms	*c*	*r*	*s*	*a*	*b*	*l*	*v*	r^2	SD[a]
untreated	3	5	−15.16	−0.041	−0.83	1.73	8.04	1.4		0.941	0.467
untreated	3-2[c]	3	−16.10			2.06	5.94	1.31		0.913	0.525
untreated	3-3[e]	3	−14.22		−1.13	-	9.83	1.15		0.923	0.49
untreated	5	5	−8.86	−0.006	−0.64	−0.05	3.68		−1.04	0.978	0.283
untreated	5-1[b]	4	−8.72		−0.65	−0.06	3.55		−1.05	0.978	0.273
untreated	5-2[d]	3	−9.12			1.18	1.12		−1.08	0.960	0.353
untreated	5-3[f]	3	−8.74		−0.64	-	3.46		−1.05	0.978	0.263
baked	3	5	−14.31	−0.016	−0.47	1.95	6.66	1.19		0.909	0.515
baked	3-2[c]	3	−14.81			2.75	5.35	1.16		0.900	0.504
baked	3-3[e]	3	−12.98		−0.89	-	8.38	1.00		0.886	0.534
baked	5	5	−8.83	0.013	−0.31	0.53	2.64		−0.93	0.975	0.270
baked	5-1[b]	4	−8.49		−0.33	0.50	2.30		−0.96	0.974	0.263
baked	5-2[d]	3	−8.69			1.13	1.07		−0.97	0.969	0.281
baked	5-3[f]	3	−8.31		−0.47		2.93		−0.93	0.972	0.263

[a] SD, the overall deviation. [b] The regression equation excluding a polarizability term from eq 5: $\log K_p = c_5 + s_5\pi_2^H + a_5\alpha_2^H + b_5\beta_2^H + v_5 \log p_L^\circ$. [c] $\log K_p = c_6 + a_6\alpha_2^H + b_6\beta_2^H + l_6 \log L^{16}$. [d] $\log K_p = c_7 + a_7\alpha_2^H + b_7\beta_2^H + v_7 \log p_L^\circ$. [e] $\log K_p = c_8 + s_8\pi_2^H + b_8\beta_2^H + l_8 \log L^{16}$. [f] $\log K_p = c_9 + s_9\pi_2^H + b_9\beta_2^H + v_9 \log p_L^\circ$.

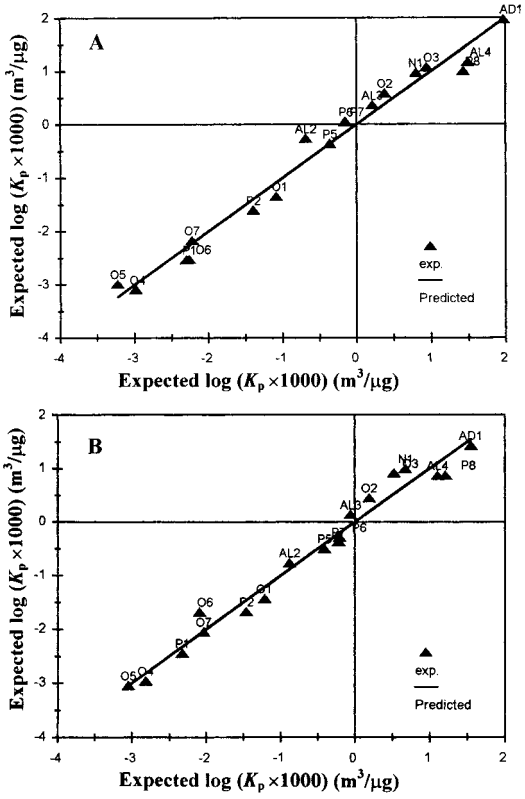

FIGURE 5. Predicted log K_p values vs experimental log K_p values (December 11, 1997) for various SOCs on two different kinds of fine Arizona road dust particles: untreated (A) and baked (B). The temperature was 282 K, and the relative humidity was 77%. The solid line is the idealized plot for the model predicted log K_p values using eq 5. Identification numbers correspond to SOCs listed in Table 2.

used herein, the discussion below shows that the correlation coefficients are consistent with the observations from the data, and this lends credence to this overall approach. It is also important to emphasize at this point that the correlation coefficients and their equations are not only a function of the adsorbent surface properties but also a function of relative humidity and temperature and, in the case of c, the specific surface area. Hence, the reported regression equations cannot be used for predictions of adsorption to other surfaces and/or other experimental conditions than those used here.

The significance of each solute scale for adsorption on the particle surface includes the chemical nature of the adsorbing active sites. As mentioned above, the SOC α_2^H and β_2^H parameters, respectively, scale the hydrogen-bonding acceptor and donator capability of the sorbant−sorbate system (*16, 17*). If graphitized carbon is used as an example substrate, one would predict that the β_2^H term for SOCs can be dropped because the adsorbing surface for SOCs predominantly plays a role as a hydrogen-bonding acceptor (*30*). Similarly, since the correlation coefficients for β_2^H parameters account for the hydrogen donation capability (*31, 32*) of active sites (e.g., silanol groups and hydroxyl groups of bounded water molecules) on dust particle surfaces, it should be highly sensitive to the baking modification imparted to inorganic dust surfaces. Model fits to the experimental data confirm this hypothesis, since the regression coefficient for the β_2^H term (*b*, in eqs 3, 5, and 5-1) was higher for untreated particles than for baked particles (Table 3).

The baking process should also increase the number of metal oxide sites through a condensation reaction of silanols on dust surfaces. For dust surfaces, the Lewis basicity (the hydrogen-bonding acceptability) described by the correlation coefficient of α_2^H of SOCs was somewhat more important in baked dust particles than in untreated dust. However, surface differences due to baking dust were reduced by ambient humidity effects as the chamber experiments proceeded. At ambient temperatures, water molecules are rapidly bound to active sites on dust surfaces (*46, 47*). In other studies, it has been observed that partitioning of SOCs decreased with increasing relative humidity, because these active sites were occupied by water molecules (*12−15, 48*). In the case of silicates, the surface is covered by a water monolayer at a relative humidity of about 30% (*10, 13*). At ambient humidities above 30%, more than a monolayer of water molecules may reside on these inorganic particle surfaces. The original surface properties of dust particles would thus be modified as a function of surface water accumulation (*49*). The removal of surface silanol groups is also considered to be reversible in the presence of water vapor (*50*). Most important, however, is the observation that the two systems approach one another as the baked system humidifies. Baking at 700 °C would most certainty drive off any preexisting organic phase and confirms that adsorptive processes are occurring for both the modified-baked and unmodified mineral dusts.

Acknowledgments

This work was supported by a Grant from the National Science Foundation to the University of North Carolina (ATM

9708533, Dr. Ann Marie Schmolther, Project Officer). We thank Bharadwaj Chandramouli and Kris Fletcher for assisting with chamber experiments.

Literature Cited

(1) Everett, D. H. *Langmuir* **1993**, *9*, 2386−2392.
(2) Pankow, J. F. *J. Chromatogr.* **1991**, *547*, 488−493.
(3) Abraham, M. H.; Walsh, D. P. *J. Chromatogr.* **1992**, *627*, 294−299.
(4) Pankow, J. F. *Atmos. Environ.* **1987**, *21*, 2275−2283.
(5) Pankow, J. F. *Atmos. Environ.* **1991**, *25A*, 2229−2239.
(6) Pankow, J. F.; Bidleman, T. F. *Atmos. Environ.* **1991**, *25A*, 2241−2249.
(7) Pankow, J. F.; Bidleman T. F. *Atmos. Environ.* **1992**, *26A*, 1071−1080.
(8) Pankow, J. F. *Atmos. Environ.* **1994**, *28*, 185−188.
(9) Storey, J. M. E.; Pankow, J. F. *Atmos. Environ.* **1992**, *26A*, 435−443.
(10) Storey, J. M. E.; Lou, W.; Isabelle, L. M.; Pankow, J. F. *Environ. Sci. Technol.* **1995**, *29*, 2420−2428.
(11) Adamson, A. W.; Gast, A. P. *Physical Chemistry of Surfaces*, 6th ed.; John Wiley & Sons: New York, 1997; pp 599−684.
(12) Goss, K. U. *Environ. Sci. Technol.* **1992**, *26*, 2287−2294.
(13) Goss, K. U. *Environ. Sci. Technol.* **1993**, *27*, 2127−2132.
(14) Goss, K. U. *Environ. Sci. Technol.* **1994**, *28*, 640−645.
(15) Goss, K. U.; Eisenreich, S. J. *Environ. Sci. Technol.* **1996**, *30*, 2135−2142.
(16) Goss, K. U. *Environ. Sci. Technol.* **1997**, *31*, 3600−3605.
(17) Goss, K. U. *J. Colloid Interface Sci.* **1997**, *190*, 241−249.
(18) Taft, R. W.; Kamlet, M. J. *J. Am. Chem. Soc.* **1976**, *98*, 2886−2894.
(19) Taft, R. W.; Abboud, J. L. M.; Kamlet, M. J. *J. Am. Chem. Soc.* **1981**, *103*, 1080−1086.
(20) Kamlet, M. J.; Taft, R. W. *J. Am. Chem. Soc.* **1976**, *98*, 377−384.
(21) Kamlet, M. J.; Taft, R. W.; Carr, P. W.; Abraham, M. H. *J. Chem. Soc., Faraday Trans. 1* **1982**, *78*, 1689−1704.
(22) Kamlet, M. J.; Abboud, J. L. M.; Abraham, M. H.; Taft, R. W. *J. Org. Chem.* **1983**, *48*, 2877−2887.
(23) Kamlet, M. J.; Abraham, M. H.; Doherty, R. M.; Taft, R. W. *J. Am. Chem. Soc.* **1984**, *106*, 464−466.
(24) Kamlet, M. J.; Doherty, R. M.; Abraham, M. H.; Marcus, Y.; Taft, R. W. *J. Phys. Chem.* **1988**, *92*, 5244−5255.
(25) Lindley, S. M.; Flowers, G. C.; Leffler, J. E. *J. Org. Chem.* **1985**, *50*, 607−610.
(26) Rutan, S. C.; Carr, P. W.; Taft, R. W. *J. Phys. Chem.* **1989**, *93*, 4292−4297.
(27) Carr, P. W. *J. Chromatogr* **1980**, *194*, 105−119.
(28) Abraham, M. H.; Whiting, G. S.; Doherty, R. M.; Shuely, W. J. *J. Chem. Soc. Perkins Trans. 2* **1990**, 1451−1460.
(29) Abraham, M. H.; Whiting, G. S.; Doherty, R. M.; Shuely, W. J. *J. Chromatogr.* **1991**, *587*, 213−228.
(30) Abraham, M. H. *J. Chromatogr.* **1993**, *644*, 95−139.
(31) Abraham, M. H. *Chem. Soc. Rev.* **1993**, *22*, 73−83.
(32) Abraham, M. H.; Haftvan, J. A.; Whiting, G. S.; Leo, A.; Taft, R. S. *J. Chem. Soc. Perkins Trans. 2* **1994**, 1777−1791.
(33) Jang, M.; Kamens, R. M.; Leach, K. B.; Strommen, M. R. *Environ. Sci. Technol.* **1997**, *31*, 2805−2811.
(34) Kamens, R. M.; Odum, J. R.; Fan, Z. *Environ. Sci. Technol.* **1995**, *29*, 43−50.
(35) Vansant, E. F.; Van Der Voort, P.; Vrancken, K. C. *Characterization and Chemical Modification of the Silica Surface;* Elsevier: New York, 1995.
(36) Dabrowski, A.; Tertykh, V. A. *Adsorption an New and Modified Inorgnic Sorbents*; Elsevier: New York, 1996.
(37) Miller, K. J.; Savchik, J. A. *J. Am. Chem. Soc.* **1979**, *101*, 7206−7213.
(38) Miller, K. J. *J. Am. Chem. Soc.* **1990**, *112*, 8533−8542.
(39) Voumard, P.; Zhan, Q.; Zenobi, R. *Langmuir* **1995**, *11*, 842−848.
(40) Yamasaki, H.; Kuwata, K.; Miyamoto, H. *Environ. Sci. Technol.* **1982**, *16*, 189−194.
(41) Yamasaki, H. K.; Kuge, Y. *Nippon Kagaku Kaishi* **1984**, *8*, 1324−1329.
(42) Tao, Y.; McMurry, P. H. *Environ. Sci. Technol.* **1989**, *23*, 1519−1523.
(43) Reid, R. C.; Prausnitz, J. M.; Poling, B. E., *The Properties of Gases and Liquids*, 4th ed.; McGraw-Hill: New York, 1987; pp 11−27 and 473−484.
(44) Schwarzenbach, R. P.; Gschwend, P. M.; Imboden, D. M. *Environmental Organic Chemistry*; John Wiley & Sons: New York, 1993; pp 72−75.
(45) Israelachvili, J. N. *Intermolecular and Surface Forces*, 2nd ed.; Academic Press: New York, 1992; pp 176−192.
(46) Dorris, G. M.; Gray, D. G. *J. Phys. Chem.* **1981**, *85*, 3628−3635.
(47) Sneh, O.; Cameron, M. A.; George, S. M. *Surf. Sci.* **1996**, *364*, 61−78.
(48) Ruiz, J.; Bilbao, R.; Murillo, M. B. *Environ. Sci. Technol.* **1998**, *32*, 1079−1084.
(49) Spange, S.; Reuter, A.; Vilsmeier, E. *Colloid Polym. Sci.* **1996**, *274*, 59−69.
(50) Gregg, S. J.; Sing, K. S. W. *Adsorption, Surface Area and Porosity*; Academic Press: London, 1982; p 272.

Received for review May 20, 1998. Revised manuscript received March 1, 1999. Accepted March 4, 1999.

ES9805167